Improving Anti-detection/interception Performance for Wireless Sensor Network Based on Time-Reversal Technology

De Li
School of Physical Electronics
UESTC
Chengdu, China
cemlab@ uestc.edu.cn

Jing-song Hong
School of Physical Electronics
UESTC
Chengdu, China
cemlab@uestc.edu.cn

Bing-zhong Wang
School of Physical Electronics
UESTC
Chengdu, China
cemlab@uestc.edu.cn

Abstract—**In recent years, wireless sensor networks (WSN) are widely applied to three-dimensional monitoring, distributed monitoring, target tracking, space exploration, a random distribution of measurement and other fields. Wireless sensor networks, such as enemy reconnaissance, strength monitoring and other special purpose on the military forces research on transmission of information security has been widely concerned. In this paper, a new technology, i.e. time reversal (TR) techniques, is utilized to reduce probability that the signal have been illegally detected in space and time. Time reversal technique allows the signal can be detected only at a specific time and specific space, while in the other time and space the signal will be very difficult to be detected; thereby TR technology will enhance the information security of wireless sensor network.**

Keywords-Time-reversal technology; Wireless sensor network; Anti-detection / interception performance; Information security

I. INTRODUCTION

At present, most of the wireless sensor network information security research focused on physical layer high-performance encryption algorithm, data link layer anti-DOS (Denial of Service) attacks on the security of MAC (Media Access Control) protocol, network layer routing of the security agreement, as well as the application layer secret key management and secure multicast [1]. Although these security measures can effectively improve the system's security，it cannot be avoided that the network information was unlawful intercepted in the process of dissemination in the space. Time-reversal technology with time-space focusing characteristic determined that only a very small space and a very narrow time frame the signal is strongest when it achieve sink node, and beyond the scope of its focus on space and time the signal is extremely weak[2]. Therefore, the time-space focusing characteristic of time-reversal technology as a novel security method can be utilized to improve security and confidentiality ability for transmitting signal in wireless sensor network instead of traditional wireless sensor network security method.
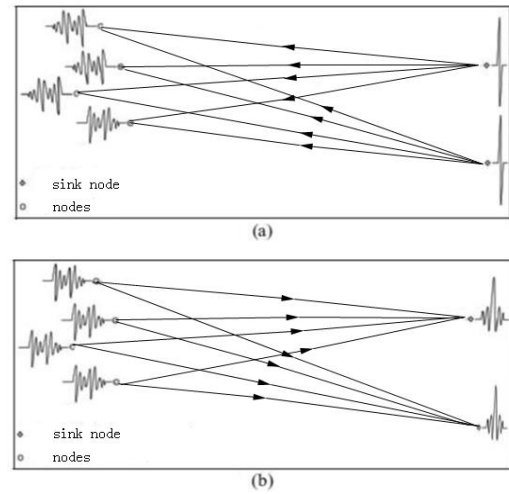
II. WSN BASED ON TR TECHNOLOGY

Fig.1 (a) *n* sink nodes transmit a short sequence of Ultra-Wideband training pulses to *m* network nodes, (b) *m* network nodes transmit time reversal signal to *n* sink nodes.

Let us consider the basic principles of MIMO WSN based on TR technology in Fig.1 [3]. Define $h_{mn}(t)$ the channel impulse response (CIR) relating the *m*-th node to the *n*-th sink node. The set of impulse responses is called the propagation operator. If one sends pulsed signal $a_m(t), m=1,...,M$ from nodes, the signal $b_n(t)$ is obtained in the *n*-th sink node as [4]

$$b_n(t) = \sum_{m=1}^{M} h_{nm}(t) * a_m(t), n=1,...,N \qquad (1)$$

Or, in matrix form,

$$\mathbf{b(t)} = \mathbf{H(t)} * \mathbf{a(t)} \qquad (2)$$

Where $\mathbf{b(t)} = [\mathbf{b_1(t), b_2(t),...,b_N(t)}]^T$,
$\mathbf{a(t)} = [\mathbf{a_1(t), a_2(t),...,a_M(t)}]^T$ and $\mathbf{H(t)}$ is the matrix of $N \times M$ with elements of $h_{nm}(t)$. The notation of " $*$ " represents element-by-element convolution; the superscript

"T" represents the conjugate transpose (Hermitian) of a vector or matrix. On the other hand, due to the spatial reciprocity, if one sends a signal $c_m(t), m=1,...,M$ from the m-th sink node, the signal $d_n(t), n=1,...,N$ is obtained in the n-th node. Defining column vectors **c** and **d** as **a** and **b**, respectively, it follows that

$$\mathbf{d(t)} = \mathbf{H^T(t) * c(t)} \tag{3}$$

As a consequence, $\mathbf{H(t)}$ permits one to calculate the forward propagation of impulses from nodes array to sink nodes, while $\mathbf{H^T(t)}$ the backward propagation from sink nodes to nodes. A time-reversal focusing is a two-step process: (1) first backward propagation and (2) then forward propagation. The two steps can be regarded as the combination of the backward propagation process described by Eq. (2) with the forward propagation process described by Eq. (3). The time-reversal process begins by sending the N × 1 vector $\mathbf{p(t)} = [\mathbf{p_1(t), p_2(t),...,p_N(t)}]^T$ from sink nodes, where $p_n(t)$ is the pulse waveform emitted from the n-th sink node. Then the signal obtained at nodes after the backward propagation is expressed according to Eq. (3) as the M x 1 vector $\mathbf{g(t)} = [\mathbf{g_1(t), g_2(t),...,g_M(t)}]^T$ given by

$$\mathbf{g(t)} = \mathbf{H^T(t) * p(t)} \tag{4}$$

where $g_n(t)$ is the pulse waveform obtained at the m-th node. In the second step, the recorded signal at nodes $\mathbf{g(t)}$ is time-reversed to yield

$$\mathbf{g(-t)} = \mathbf{H^T(-t) * p(-t)} \tag{5}$$

The time-reversed signals $g_n(-t), n=1,2,...,N$, are modulated with information-bearing pulsed waveforms $x_{km}(t), k=1,2,...,N, m=1,2,...,M$, and the resultant M pulsed waveforms corresponding to N nodes are given by

$$q_m(t) = \sum_{k=1}^{M} x_{mk}(t) * g_k(-t), m=1,...,M \tag{6}$$

Or, in matrix form,

$$\mathbf{q(t)} = \mathbf{X(t) * g(-t)} = \mathbf{X(t) * H^T(-t) * p(-t)} \tag{7}$$

Where $\mathbf{q(t)} = [\mathbf{q_1(t),...,q_M(t)}]^T$ is an N×1 vector, and the mk-th element of the M × M matrix $\mathbf{X(t)}$ is $x_{mt}(t)$. The resultant modulated signal collected in the vector $\mathbf{q(t)}$ is again re-transmitted from nodes. By combining Eq. (2), Eq. (5) and Eq. (7), the signal $\mathbf{y(t)}$ obtained at sink nodes is expressed as

$$\mathbf{y(t)} = \mathbf{H(t) * X(t) * H^T(-t) * p(-t)} \tag{8}$$

where the N × 1 vector $\mathbf{y(t)}$ has its n-th element $y_n(t)$ corresponding to the n-th sink node. $\mathbf{y(t)}$ is the signal obtained in sink nodes after time-reversal re-transmission.

III. ANTI-DETECTION / INTERCEPTION PERFORMANCE

The received signal is input to the filter followed by the squaring device and the T-second integrator as shown in Fig.2. The output of the integrator is fed to a comparator with a fixed threshold level. If the integrator output is higher than the threshold, then the signal is declared present. The performance of the radiometer is generally characterized by the probability of detection P_d (signal and noise present), the probability of false alarm P_{fa}(noise only) and the Signal power-to-Noise power spectral density S/N_0 which is a measure of the required signal power to achieve the target P_d and P_{fa} values.
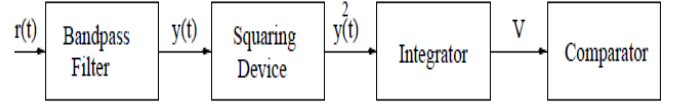

Fig.2 radiometer block diagram.

The threshold V_t of the radiometer is selected to meet the P_{fa} criterion such that the radiometer generates a false alarm when there is no signal present with probability P_{fa}. Then the S/N_0 is determined for a given Pd. Thus the required S/N_0 can be considered as a measure of covertness of the communication system of interest. When the signal is absent and the input to the radiometer is strictly additive white Gaussian noise with two-sided power spectral density $N_0/2$ and the statistics of the output of the radiometer V are normalized, then the normalized random variable $Y = 2V/N_0$ has a central chi-square distribution with $v = 2TW$ degrees of freedom where T and W are the observation time interval and the filter bandwidth of the radiometer respectively. The probability density of Y is given by[5]:

$$p_n(y) = \frac{1}{2^{v/2}\Gamma(\frac{v}{2})} y^{(v-2)/2}e^{-y/2}, y \geq 0 \tag{10}$$

When the signal is present at the input to the radiometer with energy E measured over time T, then the random variable Y has a non-central chi-square distribution with $2TW$ degrees of freedom and non-central parameter $\lambda = 2E/N_0$. The probability density of Y can then be written as[5]:

$$p_{sn}(y) = \frac{1}{2}(\frac{y}{\lambda})^{(v-2)/4} e^{-(y+\lambda)/2} I_{(v-2)/2}(\sqrt{y\lambda}), y \geq 0 \tag{11}$$

where $I_n(z)$ is the nth order modified Bessel function of the first kind. The P_{fa} and the P_d values of the radiometer can now be determined by integrating the respective conditional densities as shown:

$$p_{fa} = \int_{2V_T/N_0}^{\infty} p_n(y)dy \tag{12}$$

$$p_d = \int_{2V_T/N_0}^{\infty} p_{sn}(y)dy \tag{13}$$

Where $V_T\psi$ is the alarm threshold of the radiometer against which the output of the radiometer is compared.

In this paper, the second-order Gaussian pulse is used for the test signal, its 10dB bandwidth is 880MHz. Set simulation time step $2.5*10^{(-11)}$s as the integration time of the integrator, the probability of false alarm P_{fa} =0.001, Put P_{fa} =0.001, W=880MHz, T=2.5*10(-11)s into the above formula for calculating the relationship between P_d and SNR as shown in Fig.3. From Fig.3, it can be seen when the SNR (signal to noise ratio) is less than 96dB the signal is difficult to be detected, and when SNR is more than 116dB the probability of detection P_d equals 1.
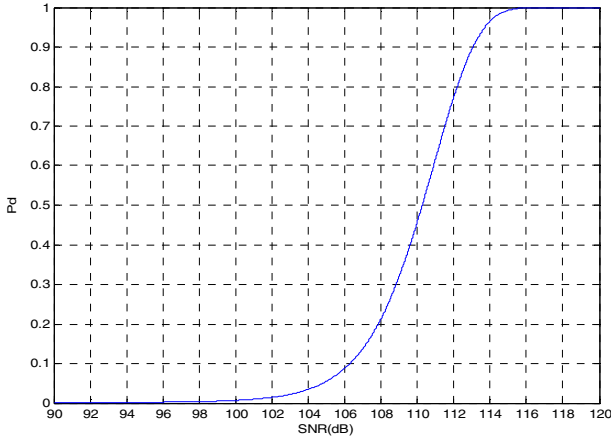

Fig.3 Probability of detection (Pd) as a function of SNR

IV. SIMULATION AND RESULTS ANALYSIS

First of all, a MISO (Multiple-Input Single-Output) system communication mode wireless sensor network as shown in Fig.4 is analyzed by simulating chamber environment for a two-dimensional simulation space (3m 6m) based on time-reversal technology in this paper. In Fig.4, the yellow point represents a sink node while green points represent nodes, and different colors represent different material objects.

FDTD method is utilized to calculate the distribution of electromagnetic in the space. In Fig.5 (a) the sink node received waveform after time reversal, near $3.2*10^{(-8)}$ s amplitude is the biggest. Let SNR=116dB when the sink node received the signal that the signal amplitude is maximum, that is P_d=1 at this very moment, as shown in Fig.3. From $SNR = 10\lg(2V/N_0)$, noise power spectral density $N_0/2$ can be gotten. In case there are signal detection devices in the space for each point, Maximum energy in the space for each time normalized by the above $N_0/2$ in Fig.5 (b), the largest SNR of space with the time curve. From Fig.5 (b) there was a peak value near $3.2\times10^{(-8)}$ s, while in the other time the signal energy distributed dispersedly, signal energy that transmitted in the space focused at this moment. For further analysis of the relationship between P_d and time, put the greatest SNR into the Eq. (13), as shown in fig.5(c). In Fig.5(c), the signal that transmitted in the space can be detected just at the moment of

time reversal focusing, while at other times the signal is very difficult to be detected out. This time are corresponded to the time that the sink node received the signal the largest amplitude. Now it is still not sure that this moment is the spatial location corresponding sink node, so space
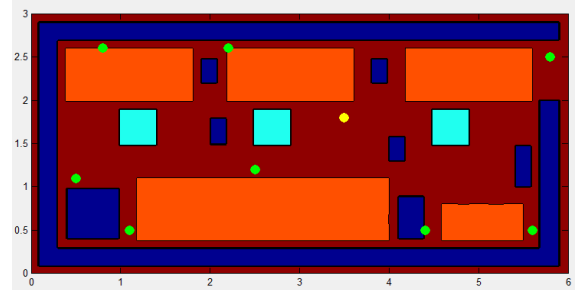
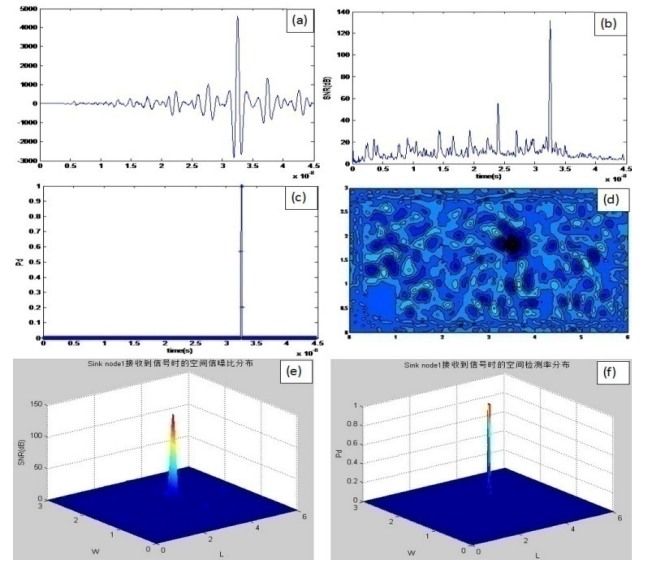

Fig.4 MISO chamber environment

Fig.5 (a) Waveform received at the sink node after time reversed propagation, (b) Largest SNR of space as a function of time after time reversed propagation (c) Probability of detection, P_d as a function of *time* after time reversed propagation, (d) Distribution of electromagnetic in the space as the sink node receive the signal, (e) Distribution of SNR in the space at the time of sink node receive the signal, (f) Distribution of probability of detection in the space at the time of sink node receive the signal

electromagnetic distribution at this moment should be gotten in order to know its corresponding spatial location. In Fig.5(d) that the space electromagnetic distribution at the moment can be found, the location of deeper color are corresponded to the sink node, description of time reversal technology makes the signal that transmitted in the space achieve spatial focusing. Spatial energy distribution at this moment can be calculated, and then spatial energy distribution normalized to the above $N_0/2$, so the SNR distribution in the entire space at this moment shown in Fig.5 (e). By Eq. (13) we can calculate the relationship between P_d and spatial location in Fig.5 (f).The signal can be detected only around the sink node a very narrow scope, while in the other place it is difficult the signal can be detected.

Secondly, a MIMO (Multiple-Input Multiple-Output) system whose structure is shown Fig.6 is analyzed in this paper. MIMO is similar to MISO, we use two-dimensional simulation space (3m × 6m) to simulate chamber environment, here two yellow points denote 2 sink nodes and nodes as shown in Fig.6. FDTD method is utilized to calculate the
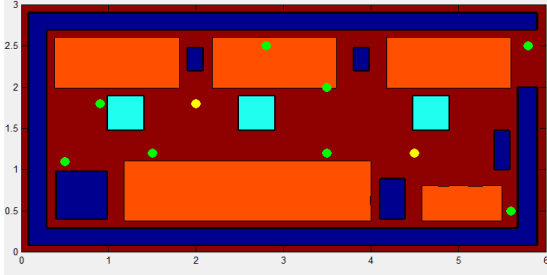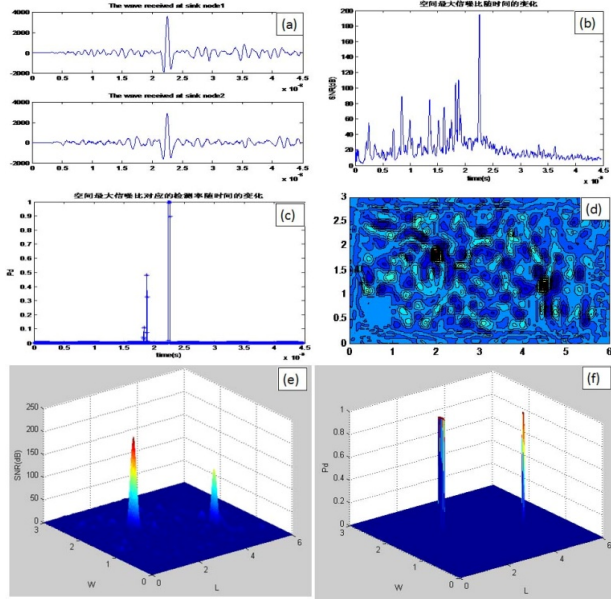

Fig.6 MIMO chamber environment

Fig.7 Waveform received at 2 sink nodes after time reversed propagation, (b) Largest SNR of space as a function of time after time reversed propagation (c) Probability of detection, Pd as a function of time after time reversed propagation, (d) Distribution of electromagnetic in the space as the sink node receive the signal, (e) Distribution of SNR in the space at the time of sink node receive the signal, (f) Distribution of probability of detection in the space at the time of sink node receive the signal

distribution of electromagnetic in the space. In Fig.7 (a) the sink node received waveform after time reversal, near $2.2*10^{(-8)}$s amplitude is the biggest. When sink nodes received the signal whose amplitude reach maximum, the smaller amplitude signal received by one of sink node is defined as SNR=116dB, that is P_d=1 at this very moment, as shown in Fig.3. By $SNR = 10\lg(2V / N_0)$, noise power spectral density $N_0/2$ can be gotten. In case there are signal detection devices in the space for each point, maximum energy in the space for each time normalized by the above $N_0/2$, the largest SNR of the space with the time curve as shown in Fig.7 (b). In Fig.7 (b) there was a peak value near $2.2\times10^{(-8)}$ s, while in the other time the signal energy distributed dispersedly, signal energy

that transmitted in the space focused at this moment. For further analysis of the relationship between P_d and time, put the largest SNR into the Eq. (13), as shown in fig.7(c). In Fig.7(c), the signal that transmitted in the space can be detected just at the moment of time reversal focusing, while in the other times the signal is very difficult to be detected out. This time are corresponded to the time that the sink node received the signal the largest amplitude. Now it is still not sure that this moment is the spatial location corresponding sink node, so if we want to know its corresponding spatial location space electromagnetic distribution at this moment should be gotten. In Fig.7(d) that the space electromagnetic distribution at the moment can be found, the location of deeper color are corresponded to the sink node, description of time reversal technology makes the signal that transmitted in the space achieve spatial focusing. Spatial energy distribution at this moment can be calculated, and then spatial energy distribution normalized to the above $N_0/2$, so the SNR distribution in the entire space at this moment shown in Fig.7 (e). By Eq. (13) we can calculate the relationship between P_d and spatial location in Fig.7 (f).The signal can be detected only around 2 sink nodes a very narrow scope, while in the other place it is difficult the signal can be detected.

From the above two sets of numerical simulations it can be seen, both the MISO and MIMO communications mode, the time-space focusing characteristic from time-reversal technology allows the signal can be detected only at a specific time and specific space, while in the other time and space the signal will be very difficult to be detected.

V. CONCLUSION

Time-reversal technology with time-space focusing characteristic can be utilized to improve information dissemination anti-detection/interception performance in the space of wireless sensor networks, reduce probability that the signal have been illegally detected in space-time domain, and improve information dissemination security in space.

REFERENCES

[1] Al-Sakib Khan Pathan, Hyung-Woo Lee, Choong Seon Hong. Security in Wireless Sensor Networks: Issues and Challenges. IEEE, Volume 2, 20-22 Feb. 2006 Page(s): 1043-1048

[2] Mathias Fink．Time Reversal of Ultrasonic Fields-Part I: Basic Principles．IEEE Transactions on Ultrasonics, Ferroelectrics, and Frequency Control, 1992, 39(5): 555-566

[3] R.J. Barton, J. Chen, K. Huang, S. Perotta and D. Wu．Optimality properties and performance analysis of co-operative time-reversal communication in wireless sensor networks．IET Commun，2007, 1 (1)：64-70

[4] Robert C. Qiu. A Theory of Time-Reversed Impulse Multiple-Input Multiple-Output (MIMO) for Ultra-Wideband (UWB) Communications. 2006 IEEE, Page(s):587-592

[5] R.F. Mills and G.E. Prescott. A Comparison of various Radiometer Detection Mod-els. IEEE Transactions on Aerospace and Electronic Systems, 1996, volume 32, page(s):467-473